Supporting Information

ROS-Scavenging Glyco-Nanoplatform for Synergistic Antibacteria and Wound-Healing Therapy of Bacterial Keratitis

Yanlong Zhang[a,b], Gang Li[a,b], Xinge Zhang[c], Ling Lin[a,b,*]

[a]State Key Laboratory of Precision Measurement Technology and Instrument, School of Precision Instruments & Opto-Electronics Engineering, Tianjin University, Tianjin 300072, China

[b]Tianjin Key Laboratory of Biomedical Detection Techniques & Instruments, Tianjin University, Tianjin 300072, China

[c] Key Laboratory of Functional Polymer Materials of Ministry of Education, Institute of Polymer Chemistry, College of Chemistry, Nankai University, Tianjin 300071, China

* Corresponding author:

E-mail: linling@tju.edu.cn (L. Lin)

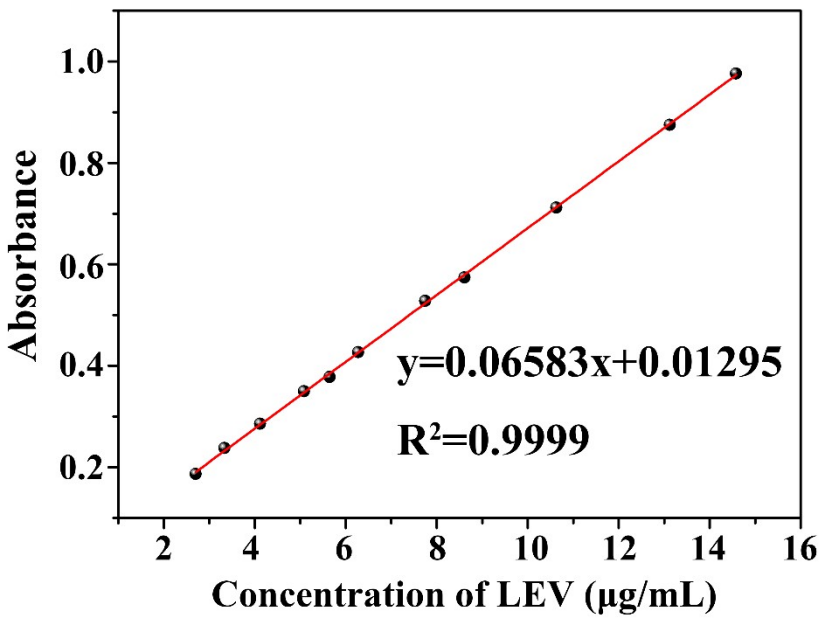

Fig. S1 The standard curve of LEV.

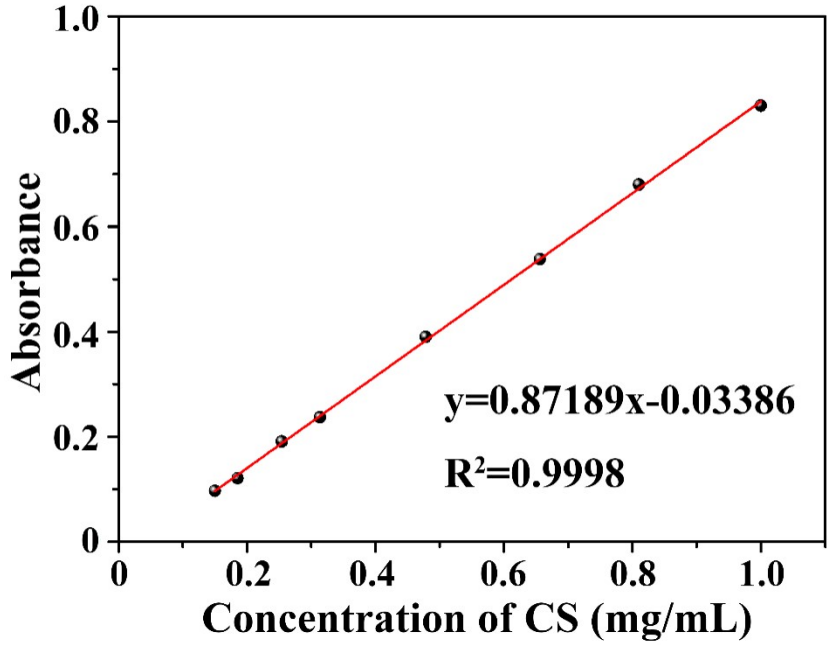

Fig. S2 The standard curve of CS.

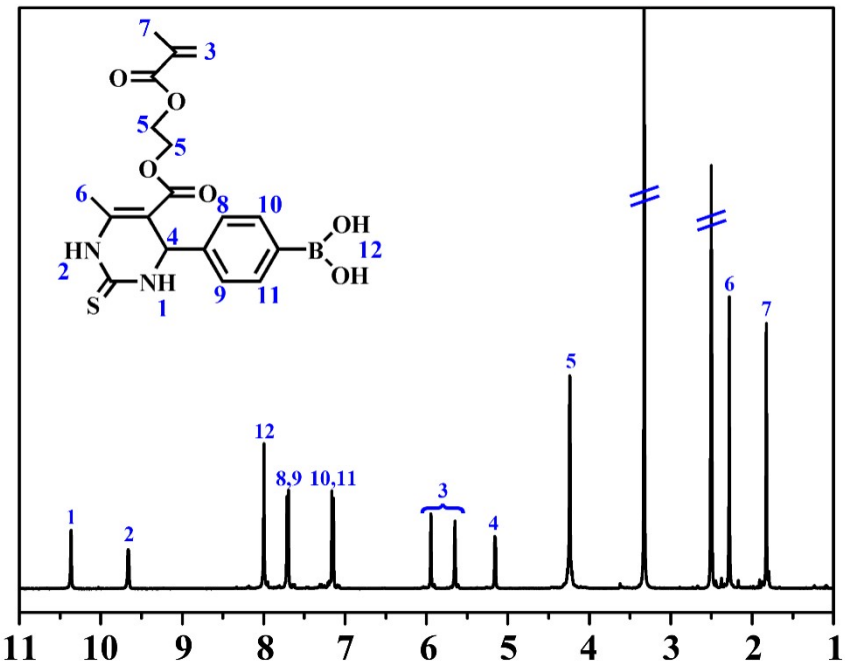

Fig. S3 ^{1}H NMR spectrum of PBA-DHPM in DMSO-d_6.

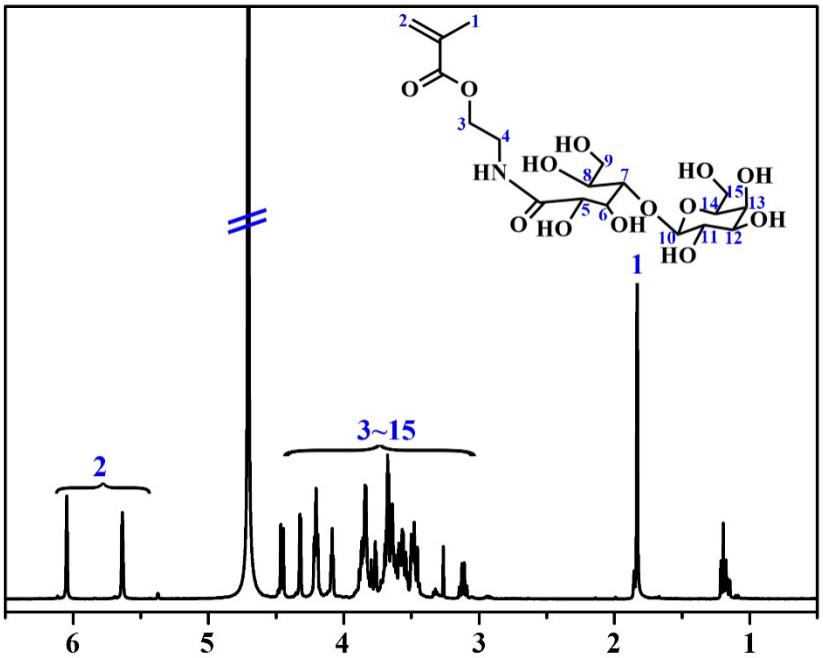

Fig. S4 ^{1}H NMR spectrum of LAMA in D_2O.

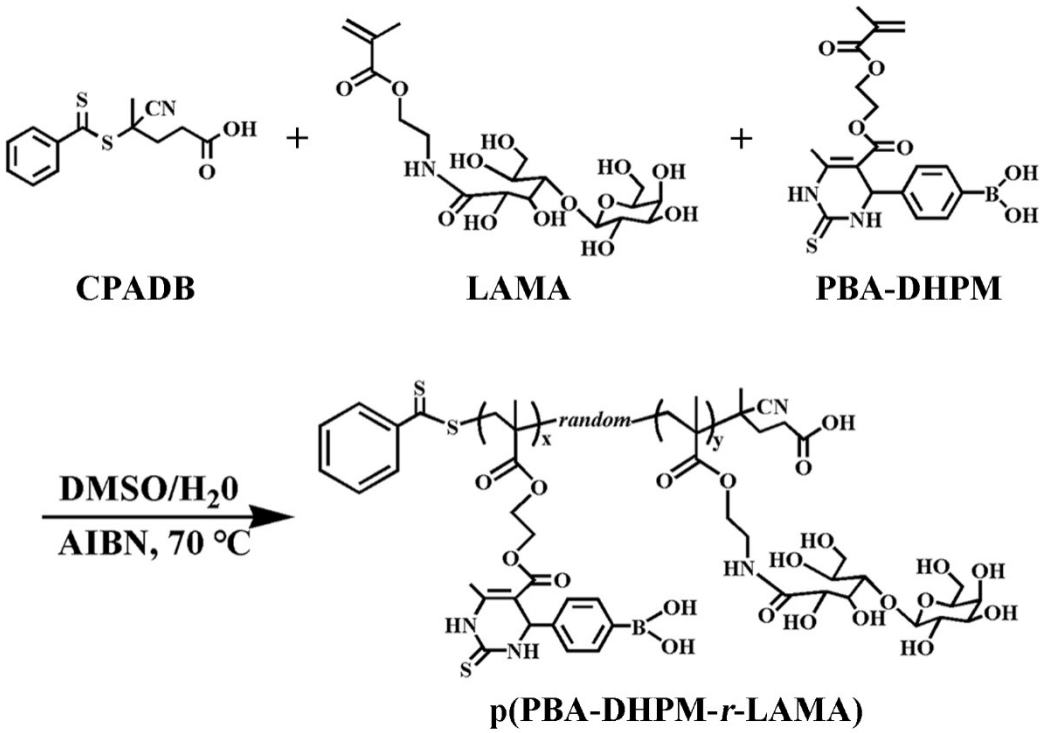

Scheme S1. Synthesis of glycopolymer p(PBA-DHPM-*r*-LAMA)

Table S1. Composition of amphiphilic glycopolymers.

Sample	Monomer		RAFT agent	Conv (wt %)[b]	PBA-DHPM/LAMA (mol/mol)	
					Theory[a]	^{1}H NMR[b]
p(PBA-DHPM$_{40}$-*r*-LAMA$_{20}$)	LAMA	PBA-DHPM	CPADB	85.43 ± 4.39	2	2.23 ± 0.16
p(PBA-DHPM$_{60}$-*r*-LAMA$_{20}$)	LAMA	PBA-DHPM	CPADB	86.76 ± 5.02	3	3.14 ± 0.19
p(PBA-DHPM$_{80}$-*r*-LAMA$_{20}$)	LAMA	PBA-DHPM	CPADB	84.74 ± 4.26	4	3.95 ± 0.21
p				>0.05		<0.05

[a]The theoretical molar ratio of PBA-DHPM/LAMA; [b]The approximate polymerization conversion and glycopolymer compositions were measured on the basis of the integral intensity of the ^{1}H NMR spectra.

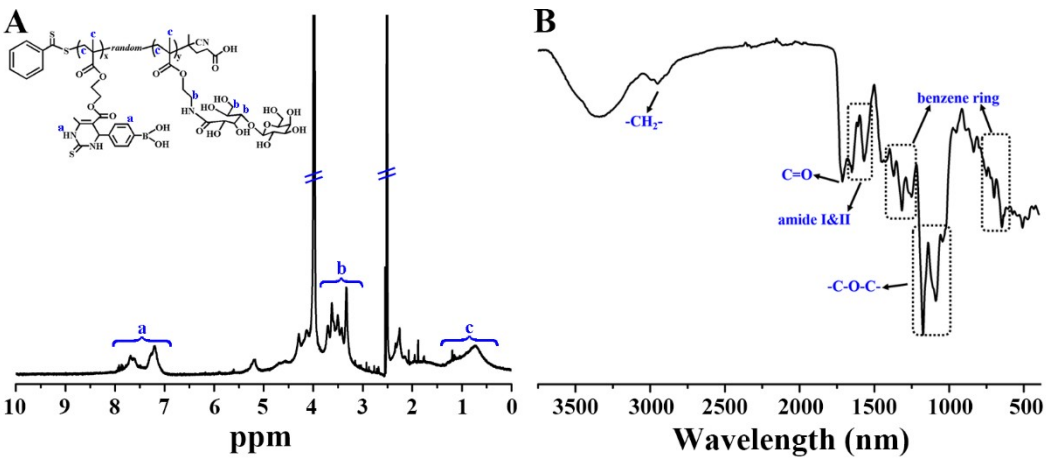

Fig. S5 (A) ^{1}H NMR (DMSO-d_6/D_2O, v/v, 4:1) and (B) FT-IR spectrum of p(PBA-DHPM-*r*-LAMA).

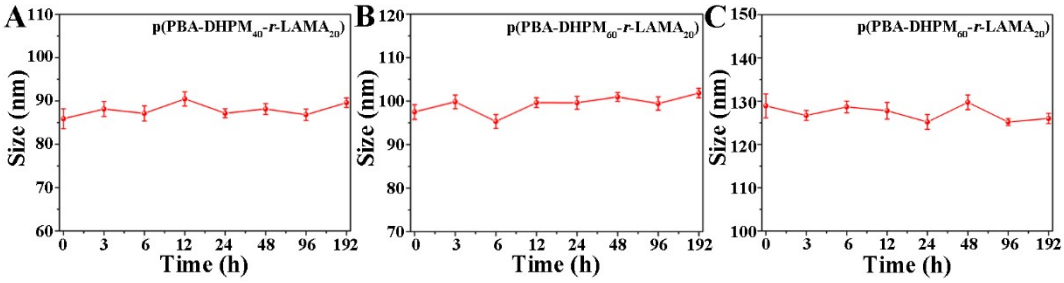

Fig. S6 Colloidal stability of (A) NP1, (B) NP2 and (C) NP3.

Table S2. D_H, PDI, zeta potential and LC of the drug-loaded glycopolymeric nanoparticles [a]

Sample	D_H (nm)	PDI	Zeta potential (mV)	LC (LEV, %)	LC (CS, %)
NP1@(C+L)	223.93 ± 6.20	0.25 ± 0.06	-18.41 ± 1.95	11.38 ± 1.46	10.46 ± 0.85
NP2@(C+L)	265.40 ± 5.45	0.22 ± 0.04	-22.32 ± 2.44	12.01 ± 2.01	12.13 ± 0.59
NP3@(C+L)	295.65 ± 8.58	0.26 ± 0.08	-31.40 ± 7.07	11.85 ± 1.82	11.57 ± 1.61
p	< 0.05	> 0.05	< 0.05	> 0.05	> 0.05

[a] Each experiment was performed in triplicate and the results were reported as mean± SD.

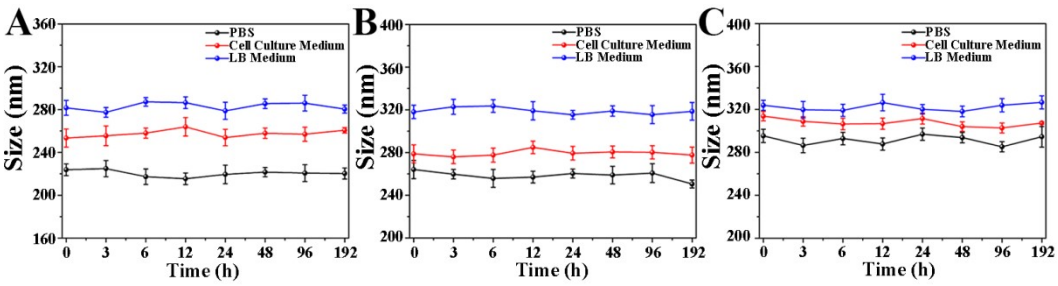

Fig. S7 Colloidal stability of (A) NP1@(C+L), (B) NP2@(C+L) and (C) NP3@(C+L) in PBS, cell culture medium and LB medium.

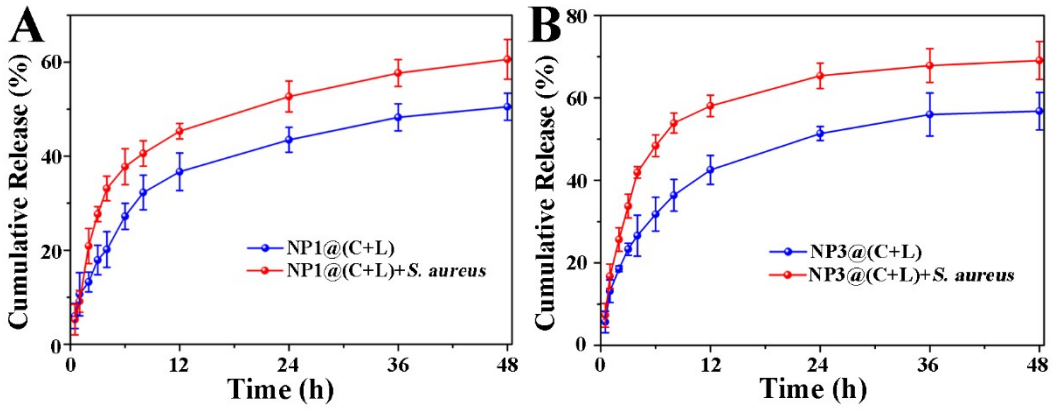

Fig. S8 *In vitro* release profiles of LEV from (A) NP1@(C+L) and (B) NP3@(C+L) nanoparticles in the absence and presence of *S. aureus* in PBS buffer (0.01 M, pH 7.4).

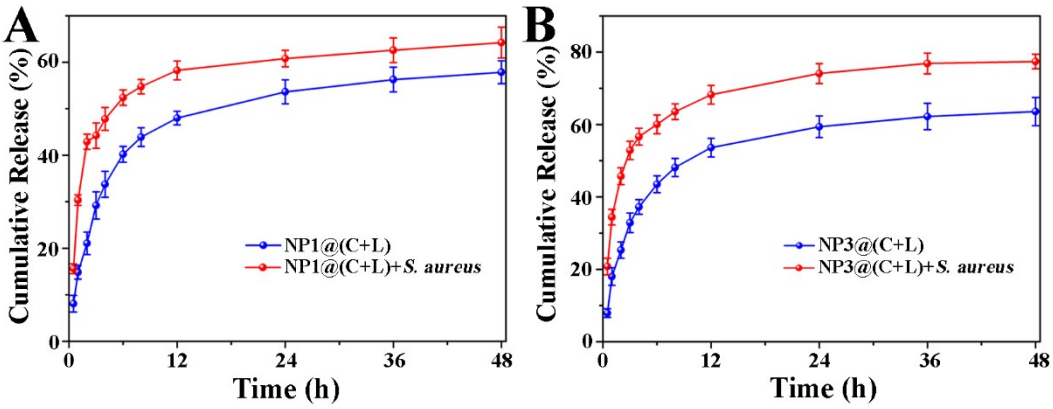

Fig. S9 *In vitro* release profiles of CS from (A) NP1@(C+L) and (B) NP3@(C+L) nanoparticles in the absence and presence of *S. aureus* in PBS buffer (0.01 M, pH 7.4).

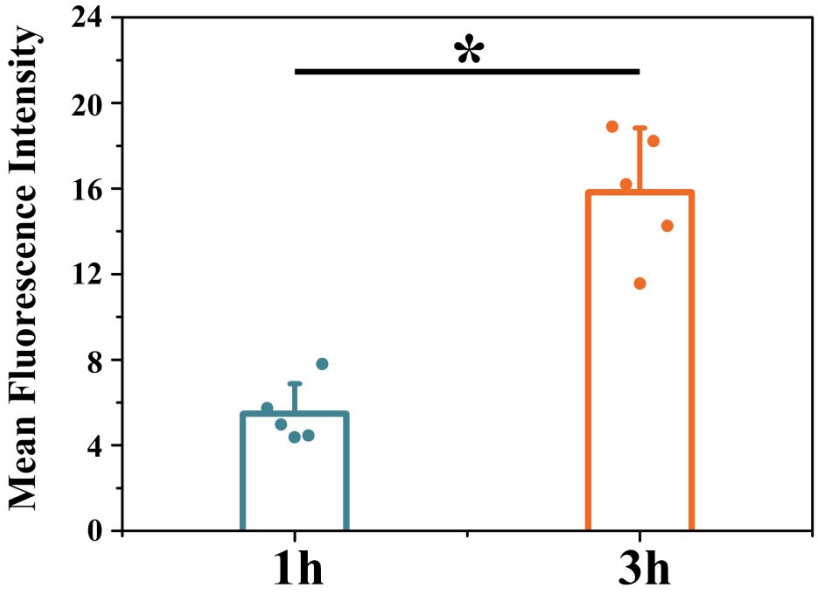

Fig. S10 Mean fluorescent intensity of internalized nanoparticles by HECEs determined by ImageJ software after incubation for 1 h and 3 h.

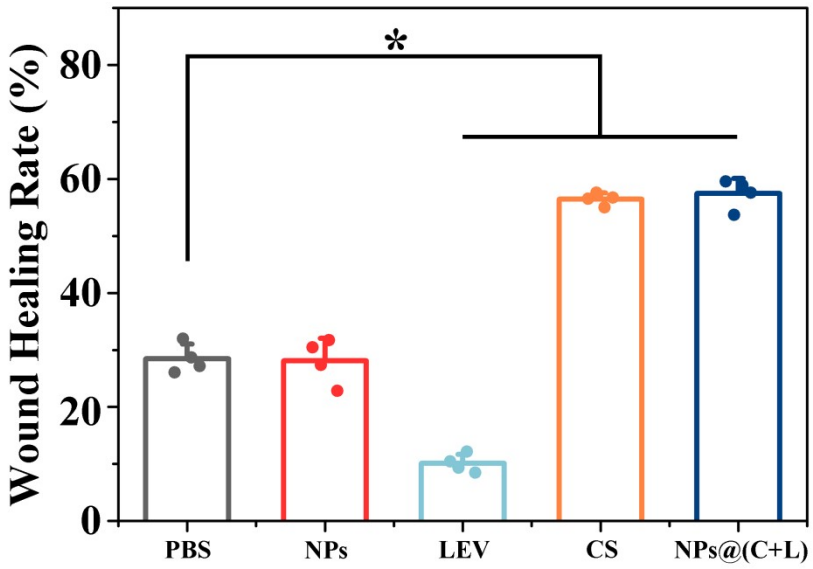

Fig. S11 Statistical analysis of wound healing rate (%).

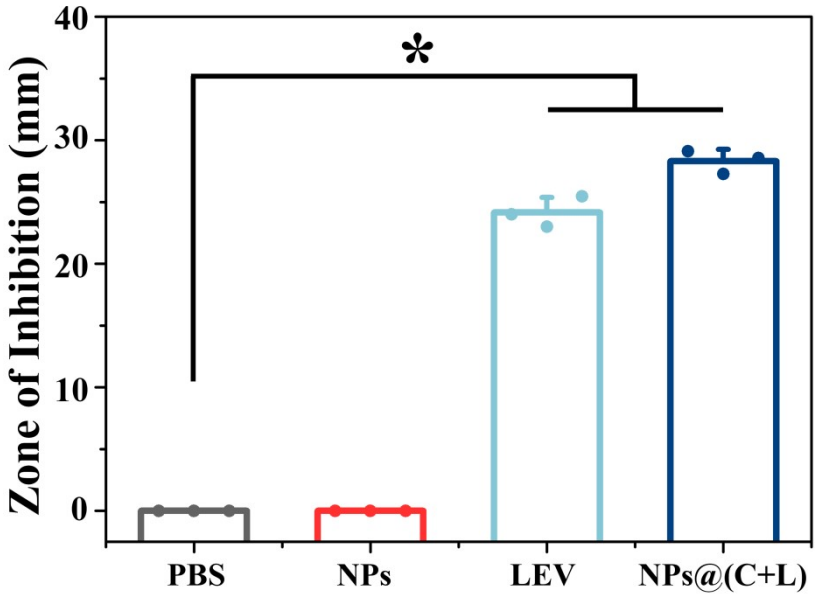

Fig. S12 Inhibition zone assay of *S. aureus* treated with PBS, NPs, LEV and NPS@(C+L).

*p<0.05.

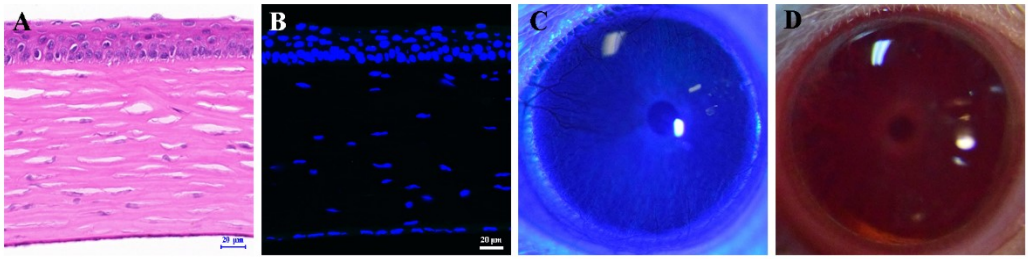

Fig. S13 (A) H&E staining, (B) fluorescence-based TUNEL staining, (C) corneal fluorescein staining, and (D) slit lamp micrograph of the corneas treated with NPs.

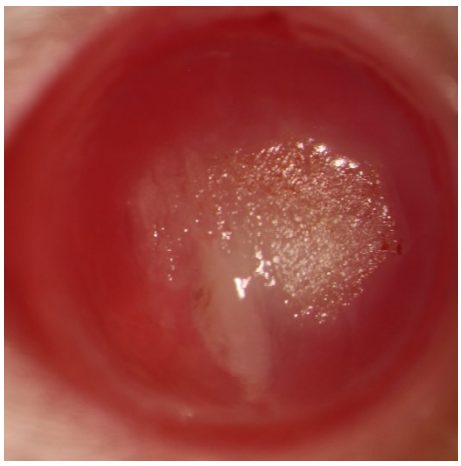

Fig. S14 The micrograph of bacterial keratitis pictured with slit lamp microscope.

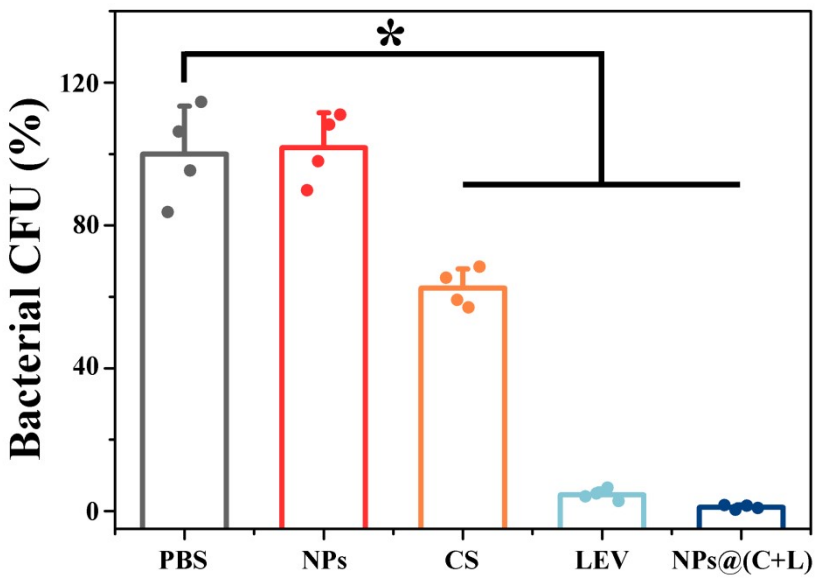

Fig. S15 Statistical analysis of bacterial CFUs on LB agar plates after treatment with PBS, NPs, LEV, CS and NPs@(C+L).

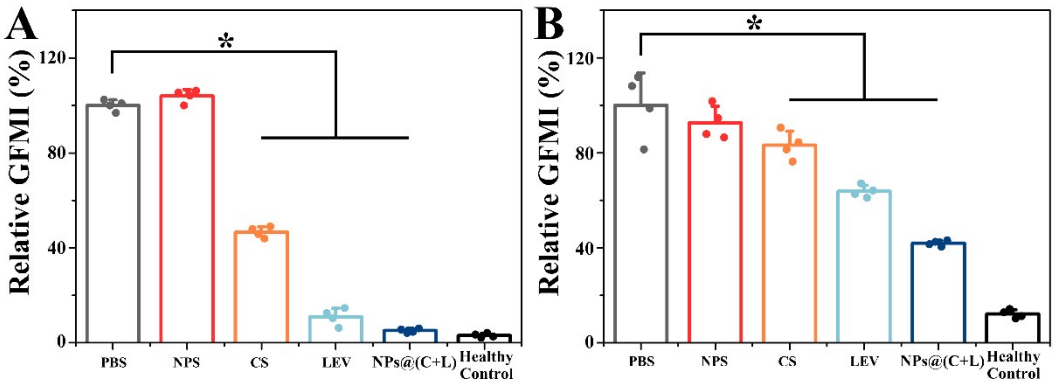

Fig. S16 Geometric fluorescent mean intensity (GFMI) of (A) IL-1β and (B) TNF-α calculated with ImageJ software. *$p < 0.05$.